The double sheath on cathodes of discharges burning in cathode vapour

2010 J. Phys. D: Appl. Phys. 43 345204

(http://iopscience.iop.org/0022-3727/43/34/345204)

IOP PUBLISHING JOURNAL OF PHYSICS D: APPLIED PHYSICS

J. Phys. D: Appl. Phys. **43** (2010) 345204 (11pp) doi:10.1088/0022-3727/43/34/345204

The double sheath on cathodes of discharges burning in cathode vapour

M S Benilov and L G Benilova

Departamento de Física, Universidade da Madeira, Largo do Município, 9000 Funchal, Portugal

Received 1 June 2010, in final form 21 July 2010
Published 12 August 2010
Online at stacks.iop.org/JPhysD/43/345204

Abstract
The model of a collisionless near-cathode space-charge sheath with ionization of atoms emitted by the cathode surface is considered. Numerical calculations showed that the mathematical problem is solvable and its solution is unique. In the framework of this model, the sheath represents a double layer with a potential maximum, with the ions which are produced before the maximum returning to the cathode surface and those produced after the maximum escaping into the plasma. Numerical results are given in a form to be readily applicable in analysis of discharges burning in cathode vapour, such as vacuum arcs. In particular, the results indicate that the ion backflow coefficient in such discharges exceeds 0.5, in agreement with values extracted from the experiment.

(Some figures in this article are in colour only in the electronic version)

1. Introduction

It was realized long ago that distributions of potential in discharges burning in cathode vapour, such as vacuum arcs and low- to high-pressure arc discharges on cathodes made of volatile materials, may possess a maximum (potential hump). For the first time it was apparently hypothesized by Plyutto *et al* [1] in order to explain the acceleration of ions towards the anode. Although by now most researchers seem to believe that the plasma acceleration in cathode jets is of a gas dynamic nature and associated with a plasma pressure gradient caused by very high pressures occurring in cathode spots (e.g. [2] and references therein), the question of potential hump in discharges burning in cathode vapour retains its significance.

A potential hump of a height approximately corresponding to the plasma temperature was revealed by modelling of the region of expansion of the cathode jet [3, 4, p 255]. This hump was attributed to the fact that the local electron pressure gradient is quite high and must be partially compensated by a retarding electric field, otherwise the electron current would be too high. In essence, this is the same mechanism that causes a negative anode voltage drop in arc discharges.

There are reasons to believe that another potential hump should exist in close proximity to the cathode surface, in a region where (cold) atoms emitted by the surface are ionized. The ions in this region are still cold and can hardly move against the electric field, in contrast to what happens in the hot plasma ball. Hence, the potential distribution in the region where ionization occurs should have a maximum, with the ions which are produced before the maximum returning to the cathode surface and those produced after the maximum escaping into the plasma.

It is of interest in this connection to try to develop a self-consistent model of the near-cathode layer in discharges burning in cathode vapour which would describe this potential maximum. It was hypothesized in [5] that such a maximum may appear in the model of a space-charge sheath if ionization of emitted atoms inside the sheath is taken into account. This model is illustrated in figure 1. There must be an inflexion point in the potential distribution positioned between the maximum point and the plasma, which means that the sheath is actually a double layer.

This model is treated in this work. Since the motion of ions in the near-cathode space-charge sheaths in discharges burning in cathode vapour is rather collision-free than collision dominated, the treatment is restricted to the case where the ions move without collisions in the sheath.

One could think of the following mechanism of formation of potential hump in this model. Let us consider two sheaths formed by collisionless cold ions and Boltzmann-distributed electrons. The flux of ions coming to the cathode, J_{iw}, is the same in both sheaths; however, in the first sheath the ions enter it from the quasi-neutral plasma with the Bohm velocity $u_{\mathrm{B}} = \sqrt{kT_{\mathrm{e}}/m_{\mathrm{i}}}$, while in the second sheath the ions are generated at rest inside the sheath. The first sheath represents the well-known Bohm model [6] and is associated with a

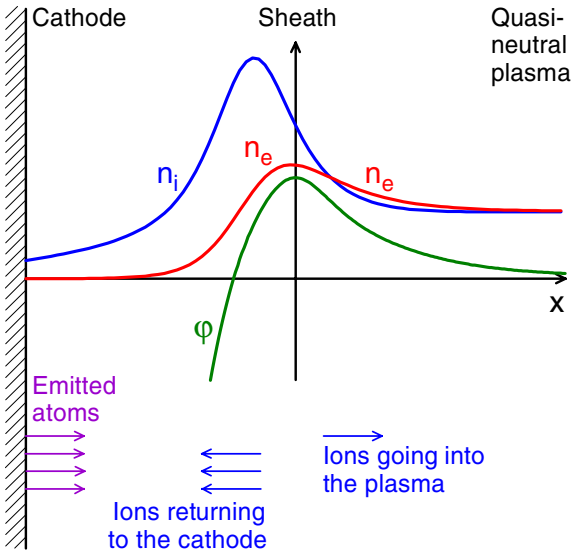

Figure 1. Schematic of a double sheath with ionization of emitted atoms.

monotonic potential distribution. The zero of potential in the first sheath is attributed to the sheath edge. One does not know at this stage whether the potential distribution in the second sheath is monotonic or non-monotonic with a maximum. If it is monotonic, the zero of potential is attributed to the sheath edge; if it is not, the zero of potential is attributed to the point of maximum. The cathode potential is the same in both sheaths.

The local density of ions at a point with a given potential φ in the first sheath is $n_{i1} = J_{iw}/v_{i1}$, where $v_{i1} = \sqrt{u_B^2 - 2e\varphi/m_i}$ is the local velocity of ions. Similarly, $n_{i2} = J_{i2}/\bar{v}_{i2}$ in the second sheath, where J_{i2} is the local ion flux and $\bar{v}_{i2}$ is the local mean ion velocity. Obviously, $J_{i2} < J_{iw}$, since a part of the ions that reach the cathode are generated between the cathode surface and the point considered and do not pass through this point. On the other hand, $\bar{v}_{i2} < \sqrt{-2e\varphi/m_i}$, since potential differences between the point being considered and the points from where the ions start at rest are below $-\varphi$. Hence, $\bar{v}_{i2} < v_{i1}$ and it may happen that $n_{i2} > n_{i1}$. If the latter is the case, the electrostatic shielding is stronger in the second sheath than in the first one, the electric filed in the second sheath decays faster and may vanish at a finite distance from the cathode, meaning a maximum of potential with subsequent reversal of the field. Of course, an accurate treatment based on a self-consistent solution of the Poisson equation is required to judge if such potential maximum can really occur.

One should mention a number of preceding works which are relevant to the problem considered. Most models of near-cathode layers in discharges burning in cathode vapour are based on the assumption that ionization of neutral atoms emitted by the cathode surface occurs in a quasi-neutral plasma region beyond the space-charge sheath and treat the sheath and the ionization region essentially in the same way as in discharges burning in the ambient gas; e.g. [2, 4, p 214, 7]. This assumption was put in question in [8, p 106] on intuitive grounds and in [5] of the basis of estimates of characteristic length scales; see also [9, figure 7.6]. Note that the conclusion [5] that this assumption may not be fulfilled is not surprising, given the very high pressures which are typical of cathode spots in discharges burning in cathode vapour and an important role that can be played by ionization in near-cathode space-charge sheaths at very high pressures [10].

Bolotov *et al* [11, 12] developed a quantitative model of potential hump in the cathode layer which has a number of similarities with the model of this work, and concluded that it offers the explanation of a number of features exhibited by vacuum arcs. However, a self-consistent solution of the Poisson equation was not attempted and a linear distribution of electric field in the cathode layer or, equivalently, a parabolic distribution of potential was assumed instead.

A double sheath occurring on cathodes with electronic emission was studied in [13, 14]; see also references therein.

The presence of a potential maximum with ions generated at rest on both sides from the maximum and moving away from it without collisions results in certain similarities between the present model and the model of Tonks and Langmuir of a collisionless positive column of a plane glow discharge enclosed by two parallel absorbing walls ([15]; see also textbooks [14, 16]). However, the potential hump in the Tonks and Langmuir model is of another nature (a consequence of symmetry) and its position is known (the axis of the discharge), in contrast to what happens in the present model. There are also similarities between the present model and models of the recycling region in tokamak scrape-off layers (e.g. [17–19] and references therein), the difference being that the space charge density in the recycling region, including in the vicinity of the potential maximum, is small.

An important feature of the present model is that the ions produced beyond the potential maximum move in the direction from the sheath into the plasma, rather than the other way round as in conventional sheath models. This feature was studied in the work [5] by means of a simple mathematical model obtained by assuming that the ionization occurs in a narrow vicinity of the point of maximum, after which the ion flux remains constant. It was found that a solution exists provided that the sheath voltage exceeds approximately $1.256kT_e/e$; a limitation similar to the one expressed by the Child–Langmuir law.

In this work, the problem of a collisionless space-charge sheath with ionization of neutral atoms emitted by the cathode is treated numerically. The outline of the paper is as follows. A mathematical model is formulated in section 2. A method of numerical solution is developed in section 3. Calculation results are given and discussed in section 4. Concluding remarks are given in section 5. The paper comprises two appendices concerned with, respectively, finding asymptotic behaviour of solution in the vicinity of the maximum of potential and estimating on the basis of available experimental information the ion backflow coefficient for the case of copper cathodes.

2. The model

2.1. Equations and boundary conditions

Let us introduce an axis x directed from the cathode surface into the plasma with the origin at point of the maximum of

electrostatic potential as shown in figure 1. Values at the cathode surface of the density of atoms emitted by the surface, n_{aw}, and of their average velocity along the x-axis, v_{a}, are considered as known parameters. In particular, if vaporization is the dominating mechanism of emission of atoms, then these parameters can be evaluated as

$$n_{\mathrm{aw}} = \frac{p_{\mathrm{v}}}{2kT_{\mathrm{w}}}, \qquad v_{\mathrm{a}} = \frac{1}{2}\sqrt{\frac{8kT_{\mathrm{w}}}{\pi m_{\mathrm{i}}}}, \tag{1}$$

where T_{w} is the temperature of the cathode surface, p_{v} is the pressure of the saturated vapour of the cathode material evaluated at the temperature T_{w} and m_{i} is the particle mass of the cathode material.

The density of flux of emitted atoms may be found as $J_{\mathrm{v}} = n_{\mathrm{aw}} v_{\mathrm{a}}$. Note that the evaluation with the use of expressions (1) gives $J_{\mathrm{v}} = p_{\mathrm{v}}/\sqrt{2\pi m_{\mathrm{i}} kT_{\mathrm{w}}}$, which is the well-known Langmuir formula.

The atoms are ionized by electron impact very rapidly, before they can collide with other atoms or the ions. Therefore, the velocity of each atom remains constant during its lifetime from emission to ionization. Since velocities of atoms, being of the order of $\sqrt{kT_{\mathrm{w}}/m_{\mathrm{i}}}$, are typically much smaller than chaotic velocities of electrons, the ionization probability does not depend on the velocity of atoms. Therefore, the velocity distribution of atoms at any point inside the sheath is the same as the velocity distribution of emitted atoms at the cathode surface. It follows that the average velocity of the atoms remains equal to v_{a}. The number density of the atoms inside the sheath is governed by the equation

$$\frac{\mathrm{d}}{\mathrm{d}x}(n_{\mathrm{a}} v_{\mathrm{a}}) = -w, \tag{2}$$

where w is the ionization rate. Equation (2) must be solved with the initial condition $n_{\mathrm{a}}(-d) = n_{\mathrm{aw}}$, where d is the distance from the cathode surface to the maximum of potential (a positive parameter to be found).

Ionization by electron impact is a dominating mechanism of ionization of neutral atoms. The estimates [9] show that electrons emitted by the cathode transfer their energy to the plasma electrons, and those produce ionization. Then the ionization term may be written as $w = k_{\mathrm{i}} n_{\mathrm{e}} n_{\mathrm{a}}$, where k_{i} is the ionization rate coefficient (a known function of the plasma electron temperature) and n_{e} is the density of plasma electrons.

Neglecting a small space charge contributed by the emitted electrons, one writes the Poisson equation as

$$\varepsilon_0 \frac{\mathrm{d}^2\varphi}{\mathrm{d}x^2} = -e(n_{\mathrm{i}} - n_{\mathrm{e}}), \tag{3}$$

where φ is the electrostatic potential and n_{i} is the ion density.

The electrostatic potential $\varphi(x)$ tends to a finite value far away from the cathode, so one can set $\varphi(\infty) = 0$. Since the origin is positioned at the point of the maximum of electrostatic potential, $\mathrm{d}\varphi/\mathrm{d}x(0) = 0$. The boundary condition at the cathode surface may be written as $\varphi(-d) = -U$, where U is a given positive parameter having the meaning of sheath voltage.

The distribution of plasma electrons is Maxwellian and their density is related to the electrostatic potential through the Boltzmann distribution

$$n_{\mathrm{e}} = n_{\mathrm{e}\infty} \exp \frac{e\varphi}{kT_{\mathrm{e}}}, \tag{4}$$

where $n_{\mathrm{e}\infty} = n_{\mathrm{e}}(\infty)$ is the electron density in the quasi-neutral plasma outside the sheath (at the 'sheath edge'); a parameter to be found. The electron temperature T_{e} is considered as a given parameter and is much higher than the cathode temperature T_{w} and much lower than eU/k.

The expression for the ion density n_{i} in the considered model is similar to the one in the Tonks–Langmuir model; however, a brief derivation is given here for completeness. Since the average momentum of an electron is much smaller than the average momentum of an atom, each ion is generated with the same velocity that the atom possessed. Therefore, if an atom possesses a kinetic energy E_{kin} and is ionized at a point $x = z$, then the ion will be generated with the total energy $E_{\mathrm{kin}} + e\varphi(z)$. Variations of electrostatic potential are of the order of kT_{e}/e in the outer section of the sheath where the densities of the ions and the electrons are comparable, and of the order of U in the inner section of the sheath where the electron density is negligible. Therefore, one can neglect the term E_{kin} (which is of the order of kT_{w}) and assume that each ion is produced with a negligible velocity and the total energy $e\varphi(z)$. We assume that the scale of the sheath thickness is much smaller than the mean free path for ion–atom collisions. Then the total energy of an ion is conserved and velocity of ions generated at a point z will be

$$v_{\mathrm{i}} = \pm\sqrt{\frac{2e}{m_{\mathrm{i}}}[\varphi(z) - \varphi(x)]} \tag{5}$$

when they have reached a point x.

The ions generated in the region $x < 0$ (i.e. between the cathode and the point of maximum of potential) move back to the cathode. The ions generated in the region $x > 0$ move into the plasma. Therefore, equation (5) should be applied either with $x < z < 0$ and the sign minus or with $0 < z < x$ and the sign plus.

The number of ions generated in the layer $z \leqslant x \leqslant z + \mathrm{d}z$ per unit time and unit area (i.e. the density of ion flux generated in this layer) is $w(z)\,\mathrm{d}z$. When the ions generated in this layer have reached a point x, their density is $w(z)\,\mathrm{d}z/|v_{\mathrm{i}}(x, z)|$. A point $x < 0$ is crossed (in the direction to the cathode) by the ions generated in the layer $[x, 0]$, a point $x > 0$ is crossed (in the direction into the plasma) by the ions generated in the layer $[0, x]$. The density of ions at a point x is

$$n_{\mathrm{i}}(x) = \int_0^x \frac{w(z)}{v_{\mathrm{i}}(x, z)}\,\mathrm{d}z. \tag{6}$$

Note that equation (6) cannot be applied directly at the point of maximum of potential, $x = 0$, since the ion velocity vanishes at $z = x = 0$. Therefore, one needs to apply the limit $x \to 0$ to equation (6) and remove the arising uncertainty in order to find $n_{\mathrm{i}}(0)$. This is done in appendix A; note that the

treatment is similar to the one in the Tonks–Langmuir model (see, e.g. appendix C of [20]).

At any $x \neq 0$, the integrand on the rhs of equation (6) has a singularity at the point $z = x$. However, the ion velocity decreases at $z \to x$ proportionally to $\sqrt{|z-x|}$, so the integral on the rhs of equation (6) converges.

2.2. *Transforming the problem*

Let us introduce the dimensionless variables:

$$\xi = \frac{x}{l_\mathrm{i}}, \qquad N_\mathrm{i} = \frac{n_\mathrm{i}}{n_\mathrm{e}^{(0)}}, \qquad N_\mathrm{a} = \frac{n_\mathrm{a}}{n_\mathrm{a}^{(0)}},$$

$$\Phi = \frac{e(\varphi - \varphi^{(0)})}{kT_\mathrm{e}}, \tag{7}$$

where $l_\mathrm{i} = v_\mathrm{a}/k_\mathrm{i} n_\mathrm{e}^{(0)}$ has the meaning of a length scale of variation of the atomic density; $n_\mathrm{a}^{(0)}$ is a characteristic value of the atomic density; $\varphi^{(0)}$ is a reference potential and $n_\mathrm{e}^{(0)} = n_{\mathrm{e}\infty} \exp \frac{\mathrm{e}\varphi^{(0)}}{kT_\mathrm{e}}$ is a parameter to be found related to $n_{\mathrm{e}\infty}$. Equations (2), (3) and (6) assume the form

$$\frac{\mathrm{d}N_\mathrm{a}}{\mathrm{d}\xi} = -\mathrm{e}^{\Phi} N_\mathrm{a}, \tag{8}$$

$$\frac{\alpha}{\tau}\frac{\mathrm{d}^2\Phi}{\mathrm{d}\xi^2} = \mathrm{e}^{\Phi} - N_\mathrm{i}, \tag{9}$$

$$N_\mathrm{i}(\xi) = \mathrm{sgn}\xi \frac{\tau}{\sqrt{2}} \int_0^\xi \frac{\mathrm{e}^{\Phi(\zeta)} N_\mathrm{a}(\zeta)}{\sqrt{\Phi(\zeta) - \Phi(\xi)}}\,\mathrm{d}\zeta, \tag{10}$$

where

$$\tau = \frac{n_\mathrm{a}^{(0)} v_\mathrm{a}}{n_\mathrm{e}^{(0)} u_\mathrm{B}}, \qquad \alpha = \frac{v_\mathrm{a}}{u_\mathrm{B}} \frac{\varepsilon_0 k T_\mathrm{e}}{n_\mathrm{a}^{(0)} e^2} \left(\frac{k_\mathrm{i} n_\mathrm{a}^{(0)}}{v_\mathrm{a}}\right)^2,$$

$$u_\mathrm{B} = \sqrt{\frac{kT_\mathrm{e}}{m_\mathrm{i}}}, \qquad \zeta = \frac{z}{l_\mathrm{i}}. \tag{11}$$

Note that $\alpha/\tau = (\lambda_\mathrm{D}/l_\mathrm{i})^2$, where $\lambda_\mathrm{D} = \sqrt{\varepsilon_0 kT_\mathrm{e}/n_\mathrm{e}^{(0)} e^2}$ is a characteristic Debye length.

The boundary conditions read in dimensionless variables as

$$N_\mathrm{a}(\xi_\mathrm{w}) = N_\mathrm{aw}, \qquad \Phi(\xi_\mathrm{w}) = -\chi - \chi_1, \qquad \frac{\mathrm{d}\Phi}{\mathrm{d}\xi}(0) = 0,$$

$$\Phi(\infty) = -\chi_1, \tag{12}$$

where $\xi_\mathrm{w} = -d/l_\mathrm{i}$ is the value of the coordinate ξ corresponding to the cathode surface, $N_\mathrm{aw} = n_\mathrm{aw}/n_\mathrm{a}^{(0)}$, $\chi = eU/kT_\mathrm{e}$, $\chi_1 = e\varphi^{(0)}/kT_\mathrm{e}$.

Equations (8)–(10), (12) represent the statement of the problem in dimensionless variables. Note that parameters τ and ξ_w are unknown and must be found as a part of solution.

The normalization parameters $n_\mathrm{a}^{(0)}$ and $\varphi^{(0)}$ will be set equal to values at the point of maximum. In other words, it is assumed $n_\mathrm{a}^{(0)} = n_\mathrm{a}(0)$, $\varphi^{(0)} = \varphi(0)$, so that

$$N_\mathrm{a}(0) = 1, \qquad \Phi(0) = 0. \tag{13}$$

The order of the system of equations can be reduced by one. To this end, let us substitute equation (10) into equation (9), multiply the obtained equation by $\mathrm{d}\Phi/\mathrm{d}\xi$, and integrate over ξ from 0 to ξ. After the order of integration over ξ and ζ in the double integral on the rhs has been changed, the integral over ξ may be evaluated analytically. Taking into account the third boundary condition (12) and the second boundary condition (13), one obtains

$$\frac{\mathrm{d}\Phi}{\mathrm{d}\xi} = -\mathrm{sgn}\xi \sqrt{\frac{2\tau}{\alpha}} [\mathrm{e}^{\Phi} - 1 + \mathrm{sgn}\xi \sqrt{2}\tau I(\xi)]^{1/2}, \tag{14}$$

where

$$I(\xi) = \int_0^\xi \mathrm{e}^{\Phi(\zeta)} N_\mathrm{a}(\zeta) \sqrt{\Phi(\zeta) - \Phi(\xi)}\,\mathrm{d}\zeta. \tag{15}$$

3. Method of numerical solution

While solving the problem numerically, it is convenient to treat the atomic density at the point of maximum, $n_\mathrm{a}(0)$, as a given parameter, and the atomic density at the cathode surface, n_aw, as a calculation result. Then the solution may be found in two steps. First, equations (8) and (14) are solved for functions $N_\mathrm{a}(\xi)$ and $\Phi(\xi)$ and constant τ in the region beyond the maximum point, $\xi \geqslant 0$, the boundary conditions being (13) and

$$\frac{\mathrm{d}\Phi}{\mathrm{d}\xi}(\infty) = 0. \tag{16}$$

After the solution has been found, one will be able to determine the constant χ_1: $\chi_1 = -\Phi_\infty$, where $\Phi_\infty = \Phi(\infty)$.

At the second step, equations (8) and (14) are solved for functions $N_\mathrm{a}(\xi)$ and $\Phi(\xi)$ and constant ξ_w in the layer between the cathode and the maximum point, $\xi_\mathrm{w} \leqslant \xi < 0$, with the boundary conditions (13) and the condition $\Phi(\xi_\mathrm{w}) = -\chi + \Phi_\infty$.

The first problem represents a two-point boundary-value problem for two equations, one of these equations being (ordinary) differential and the other integrodifferential. It is natural to try to solve it by shooting with τ playing the role of a shooting parameter: equations (8) and (14) supplemented with boundary conditions (13) are integrated from the point $\xi = 0$ in the direction of positive ξ; the integration is performed several times with different values of parameter τ and this parameter is adjusted until the boundary condition (16) or an equivalent condition is satisfied. The second problem also represents a two-point boundary-value problem; however, it can be trivially reduced to an initial-value problem: equations (8) and (14) supplemented with boundary conditions (13) are integrated from $\xi = 0$ in the direction of negative ξ; the integration terminates when the function Φ attains the value $-\chi + \Phi_\infty$.

The above-described procedure requires a numerical solution of the initial-value problem (8), (14), (13) with a known τ. After an appropriate method of evaluation of integral (15) has been chosen, equations (8) and (14) with boundary conditions (13) may be treated as an initial-value problem for a system of two first-order ordinary differential equations. In this work, these equations were solved by means of Euler's method on a numerical grid with a constant step h. Potential at the first knots, $\xi = \pm h$, was determined by means of equation (22)

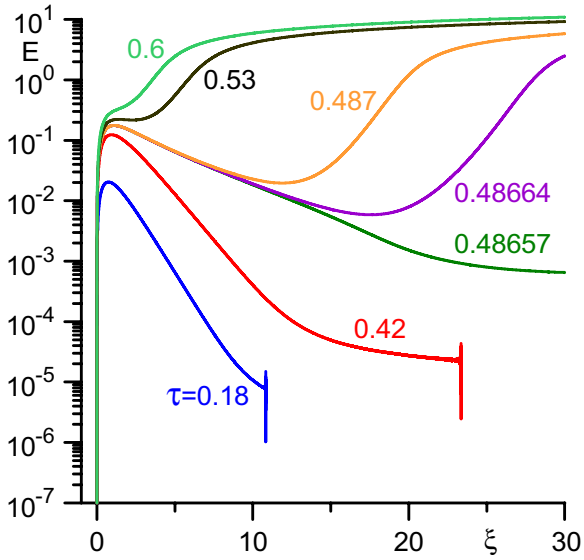

Figure 2. Distribution of the electric field in the region beyond potential hump. $\alpha = 0.1$, $h = 10^{-3}$.

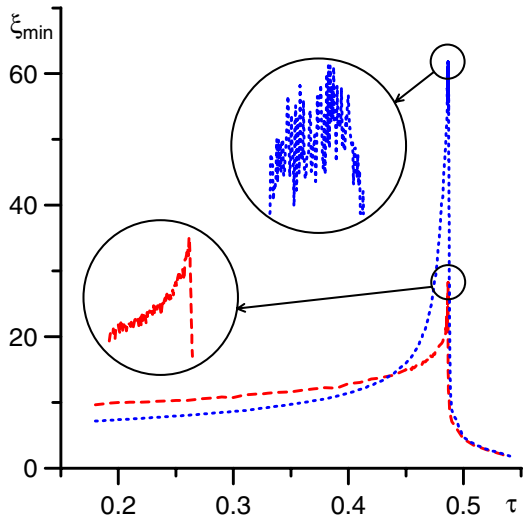

Figure 3. First minimum of the distribution of electric field in the region beyond potential hump. $\alpha = 0.1$. Dotted: $h = 10^{-2}$. Dashed: $h = 10^{-3}$.

Table 1. Values of τ which ensure the longest interval of monotonic decrease in electric field.

	α		
h	0.1	1	10
10^{-2}	0.48 668	0.47 897	0.46 164
10^{-3}	0.48 657	0.47 795	0.46 014

of appendix A supplemented with the rest of equations of the appendix.

The boundary condition (16) does not admit a straightforward numerical implementation, so an equivalent numerical condition is needed to find τ. As an example, let us consider the results of numerical solution of the initial-value problem (8), (14), (13) in the region $\xi \geqslant 0$ with different values of τ for $\alpha = 0.1$ and $h = 10^{-3}$. If $\tau \lesssim 0.17$, the numerical solution breaks down at the third knot of the numerical grid, $\xi = 3h$, where the quantity in the square brackets in equation (14) turns negative. Calculated distributions of the dimensionless electric field $E = -\mathrm{d}\Phi/\mathrm{d}\xi$ for several values of $\tau \geqslant 0.18$ are shown in figure 2. At $\tau = 0.18$, the electric field $E(\xi)$ first increases, then passes through a maximum at $\xi = \xi_{\max} = 0.735$, then passes through a minimum at $\xi = \xi_{\min} = 9.592$ after which it starts rapidly oscillating. The amplitude of the oscillations, being very low at ξ close to $\xi_{\min}$, increases with increasing ξ. At ξ around 10.8 the oscillations become visible on the graph and at $\xi = \xi_{\mathrm{bd}} = 10.828$ the solution breaks down (for the same reason as above: the quantity in the square brackets in equation (14) turns negative). At $\tau = 0.42$ the distribution $E(\xi)$ is qualitatively similar, except that the first maximum, the first minimum and the point of breakdown have shifted to higher ξ: $\xi_{\max} = 0.930$, $\xi_{\min} = 13.466$, $\xi_{\mathrm{bd}} = 23.369$. At $\tau = 0.48\,657$ the first maximum has shifted a little bit more: $\xi_{\max} = 1.087$, the first minimum has shifted considerably: $\xi_{\min} = 28.256$, and the solution exists in the whole calculation domain (which was $0 \leqslant \xi \leqslant 30$). There are still over a hundred cycles of oscillation of $E(\xi)$ in the region $\xi_{\min} \leqslant \xi \leqslant 30$; however, the amplitude of the oscillations is quite low and they are not visible on the graph. As τ increases further, $\xi_{\min}$ starts decreasing; however, the solution continues to exist in the whole calculation domain while the number of cycles of oscillations in the region $\xi_{\min} \leqslant \xi \leqslant 30$ decreases. At $\tau = 0.48\,664$, $\xi_{\max} = 1.088$ and $\xi_{\min} = 17.563$ and there are no oscillations of $E(\xi)$ in the region $\xi_{\min} \leqslant \xi \leqslant 30$, i.e. the electric field is monotonically increasing in this region. At $\tau = 0.487$ the distribution $E(\xi)$ is qualitatively similar, except that the minimum has shifted still more in the direction of lower ξ: $\xi_{\max} = 1.089$ and $\xi_{\min} = 11.897$. At $\tau = 0.53$ the distribution $E(\xi)$ is still qualitatively similar; however, the maximum and the minimum are relatively close: $\xi_{\max} = 1.375$, $\xi_{\min} = 2.293$, and that the electric field in the region $[\xi_{\max}, \xi_{\min}]$ does not change much: $E(\xi_{\max}) \approx 0.223$, $E(\xi_{\min}) \approx 0.218$. At τ still higher the maximum and the minimum disappear, so $E(\xi)$ monotonically increases in the whole calculation domain, an example being the case $\tau = 0.6$.

It is legitimate to assume that the proper value of τ in this example is 0.48 657, i.e. the one which ensures the biggest $\xi_{\min}$ or, in other words, the longest interval of monotonic decrease in electric field after the first maximum. This assumption is illustrated in figure 3, where the quantity $\xi_{\min}$ for $\alpha = 0.1$ is shown as a function of τ for two values of h, and by table 1, where values of τ are shown which ensure the biggest $\xi_{\min}$ for different (α, h), $\alpha = 0.1$, 1, 10 and $h = 10^{-2}$, 10^{-3}. The maximum in the dependence $\xi_{\min}(\tau)$ is quite narrow and the variation of its position with h is quite weak, which leaves little doubt concerning the problem under consideration being solvable and its solution being unique.

In the case $h = 10^{-2}$, the dependence $\xi_{\min}(\tau)$ is oscillating in the vicinity of maximum, as seen in the upper inset in figure 2. This causes a small ambiguity in the choice of τ. There is no such ambiguity in the case $h = 10^{-3}$; however, $\xi_{\min}$ in the vicinity of maximum in this case is substantially lower than in the case $h = 10^{-2}$; probably an indication of

accumulation of error. These factors affect the accuracy of the numerical procedure being used. It will be seen below that this accuracy may be estimated as about 10%.

4. Results and discussion

Examples of calculated distributions of parameters in the sheath are shown in figure 4; here $N_e = e^{\Phi}$ is the normalized electron density. The ion density was found from the Poisson equation (9) with the use of numerical differentiation of E. There are small oscillations of the ion density in the vicinity of the point of maximum of potential, which are not very visible on the graph in the case $\alpha = 0.1$, virtually invisible in the case $\alpha = 1$, and not visible at all in the case $\alpha = 10$. These oscillations represent a numerical artefact. There is a difference of up to 10% between solutions obtained on different numerical grids, which gives an idea of the overall accuracy of numerical results.

One can see that the numerical results confirm the physical picture hypothesized in the introduction. There is a maximum in the distribution of potential and, consequently, of the electron density. There is a maximum also in the distribution of the electric field, $\xi = \xi_{max}$, at which the ion and electron densities become equal. N_i exceeds N_e at $\xi < \xi_{max}$ and is below N_e at $\xi > \xi_{max}$; a double layer. The ion density is non-monotonic as well, with a maximum positioned at a negative ξ.

The modelling reported in this work refers to the case $\chi = 10$; in other words, the integration in the direction of negative ξ terminated when the potential has decreased to $-10kT_e/e$. Values of ξ at which this happened, i.e., position of the cathode, $\xi = \xi_w$, are shown in table 2. The density (and flux) of atoms emitted by the cathode surface remains unaltered in the vicinity of the cathode, where the plasma is strongly negative and from where the electrons are repelled by the sheath electric field, so no ionization occurs. Further away from the cathode, the electron density becomes appreciable and atoms start getting ionized: N_a starts decreasing. In order to give an idea of a region where this happens, values $\xi = \xi_1$ at which N_e reaches the value of 10^{-2} are shown in table 2.

As ξ increases, the atomic density decreases rather fast and soon becomes negligible, i.e. the plasma becomes fully ionized. In order to give an idea of a region where this happens, values $\xi = \xi_2$ at which N_a decreases down to 1% of the value at the cathode surface (i.e., 99% of the atoms have been ionized) are shown in table 2. Also shown in table 2 are values $\xi = \xi_i$ at which N_i attains a maximum. As it should have been expected, $\xi_1 < \xi_i < \xi_2$: the maximum of ion density occurs inside the ionization zone.

At $\alpha = 0.1$, the ion density in the region of the potential hump is relatively close to the electron density, so the plasma is not very far from quasi-neutrality here. With increasing α the ion density in the region of the potential hump increases and at large α considerably exceeds the electron density.

Another important quantity is the average potential energy with which ions crossing a point x have been produced:

$$\psi_i(x) = \frac{1}{[n_a(0) - n_a(x)]v_a} \int_0^x we\varphi \, dx. \qquad (17)$$

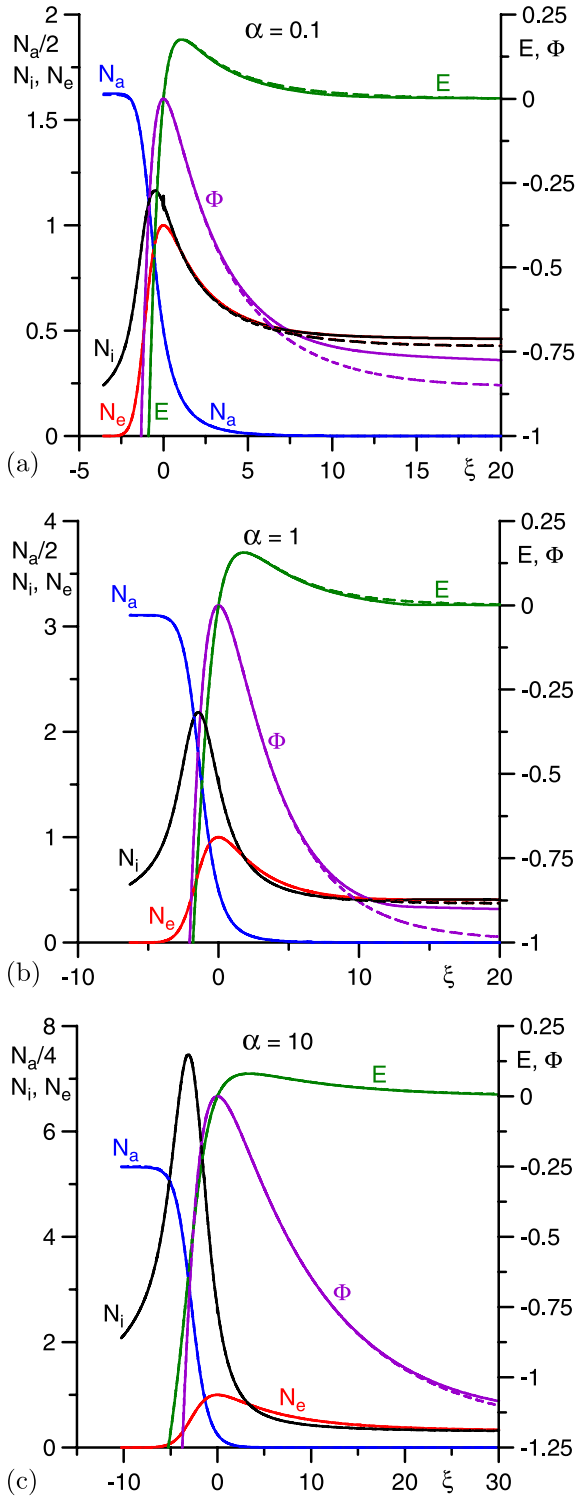

Figure 4. Distribution of ion, electron and atomic densities, electrostatic potential and electric field across the sheath. Solid: $h = 10^{-2}$. Dashed: $h = 10^{-3}$.

The average kinetic energy of an ion at a point x can be expressed in terms of this quantity as $\psi_i(x) - e\varphi(x)$. A dimensionless average potential energy may be conveniently defined as $\Psi_i = \psi_i/kT_e + \Phi_\infty$ and equals

$$\Psi_i(\xi) = \frac{1}{1 - N_a} \int_0^\xi e^{\Phi} N_a \Phi \, d\xi. \qquad (18)$$

Distributions of the function $\Psi_i(\xi)$ are shown in figure 5(*a*). As one should have expected, the function attains a maximum value $\Psi_i = 0$ at $\xi = 0$ and manifests plateaus in the region $\xi \lesssim \xi_1$, where no ionization occurs, and in the region $\xi \gtrsim \xi_2$, where the plasma is already fully ionized.

Equation (14) in the region $\xi \lesssim \xi_1$, where the electron density is negligible and no ionization occurs, may be written as

$$\frac{\alpha}{2\tau}\left(\frac{d\Phi}{d\xi}\right)^2 = \sqrt{2}\tau \int_{\xi}^{0} e^{\Phi(\zeta)} N_a(\zeta)\sqrt{\Phi(\zeta) - \Phi(\xi)}\, d\zeta - 1. \tag{19}$$

Note that the lower limit of integration may be set equal, instead of ξ, to any value below ξ_1.

Modulus of potential in the region in the vicinity of the hump, where ionization occurs, is of the order of kT_e/e. Modulus of potential in the region $\xi \lesssim \xi_1$ is of the order U, i.e. substantially higher. Therefore, the integrand on the rhs of equation (19) may be expanded in powers of $\Phi(\zeta)/\Phi(\xi)$. Retaining two terms of the expansion, one finds

$$\frac{\alpha}{2\tau}\left(\frac{d\Phi}{d\xi}\right)^2 = \tau(N_a - 1)\sqrt{-2\Phi}\left(1 - \frac{\Psi_i}{2\Phi}\right) - 1. \tag{20}$$

While equation (19) is of exponential accuracy with respect to the large parameter $-\Phi$, equation (20) is of only algebraic accuracy $O(\Phi^{-2})$. Nevertheless, equation (20) is accurate enough, which is illustrated by graphs of the ratio of the lhs of this equation to the rhs shown in figure 5(*a*). One can see that in the region $\xi \lesssim \xi_1$ this ratio indeed is close to unity. The fact that the asymptotic limit of validity of equation (20) is related to the large parameter $-\Phi$ is illustrated in figure 5(*b*), where the data referring to the range $\xi \leqslant 0$ in figure 5(*a*) are plotted versus Φ.

Table 2. Position of the cathode, boundaries of a zone where ionization occurs, position of the maximum of ion density.

	α		
	0.1	1	10
ξ_w	−3.6	−6.3	−10.3
ξ_1	−2.4	−4.0	−6.5
ξ_2	4.6	3.3	1.6
ξ_i	−0.5	−1.4	−3.1

Integral parameters of the sheath for different values of α are shown in figure 6. Here $\Psi_{iw} = \Psi_i(\xi_w)$ and $\Psi_{i\infty} = \Psi_i(\infty)$ are dimensionless average potential energies with which ions have been produced before and after the potential maximum, respectively. Data calculated on different numerical grids are rather close to each other except for Φ_∞ where the difference is more substantial and the dependence on α is not smooth, especially when calculated with $h = 10^{-2}$; clearly a consequence of the numerical difficulties discussed at the end of section 3. However, the difference is below 10% even in this case, which is an acceptable accuracy at the present stage.

It is of interest to try to find an asymptotic solution to the considered problem in the limiting cases of small and large α. Leaving the full treatment beyond the scope of this paper, we note the following. Values of the quantities τ and Φ_∞ in the case of large α can be found with the use of results [5]: $\Phi_\infty = -C_1$, where $C_1 \approx 1.26$ is the positive root of the transcendental equation $\exp C_1 = 1 + 2C_1$, and $\tau = \sqrt{2C_1}/(1 + 2C_1) \approx 0.451$.

In the limiting case of small α, the space charge and ionization are separated in space: the ionization occurs in a quasi-neutral region beyond the space-charge sheath, which may be called the ionization layer. The sheath is formed by ions returning to the cathode and is not very different from sheaths in discharges burning in ambient gas. While the potential distribution in the sheath is monotonic in this limiting case, the maximum of potential occurs in the ionization layer. Therefore, the ionization layer in discharges burning in cathode vapour is substantially different from that in discharges burning in ambient gas. To the first approximation in the parameter α, the ionization layer is described by a problem comprising equation (8), equation (9) with the lhs being dropped, and boundary condition (13) and (16). This problem

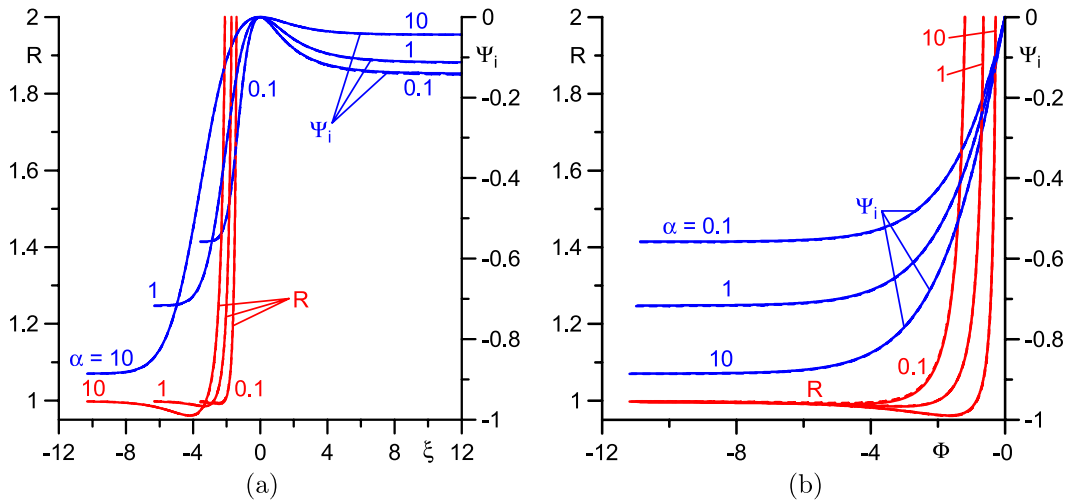

Figure 5. Ψ_i: dimensionless average potential energy with which ions crossing a point ξ have been produced. R: ratio of the lhs of equation (20) to the rhs. Solid: $h = 10^{-2}$. Dashed: $h = 10^{-3}$.

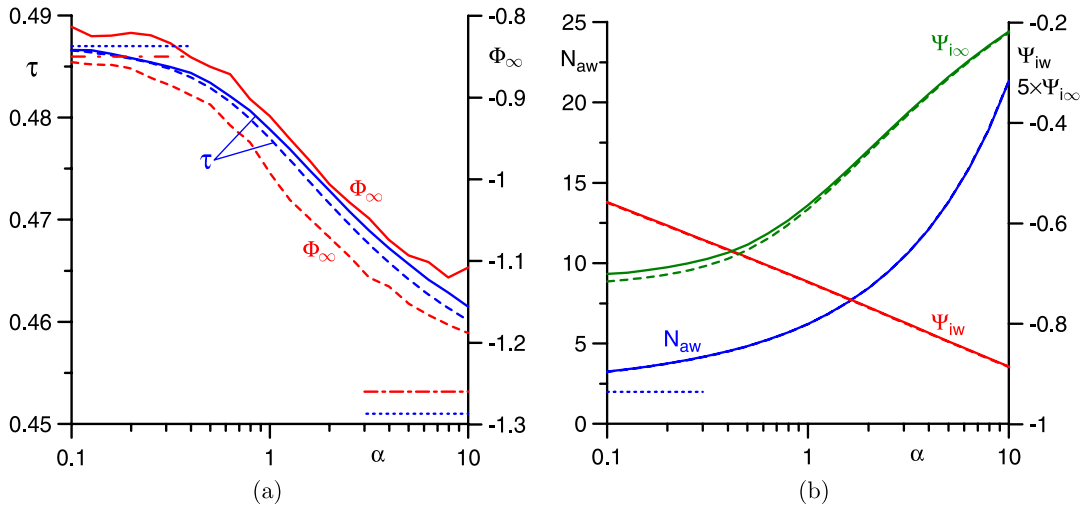

Figure 6. Integral parameters of the sheath. Solid: $h = 10^{-2}$. Dashed: $h = 10^{-3}$. Dotted and dashed–dotted: asymptotic behaviour for small or large α.

may be solved analytically similarly to how it was done in the model of Tonks and Langmuir of a collisionless plane glow discharge under the assumption of quasi-neutrality [21]. However, the obtained solution is not unique: there is a one-parameter family of solutions. It is unclear which procedure of choosing one solution from this family is the most adequate; for example, stability considerations have been invoked in a similar problem [19]. Without discussing this question, we will choose the limiting solution, which is the one associated with the highest possible potential hump. In the framework of this solution, $\tau = \sqrt{2}/\pi\eta_{\rm m} \approx 0.487$, $\Phi_\infty = -\eta_{\rm m}^2 \approx -0.854$, and $N_{\rm aw} = 2$. (Here $\eta_{\rm m} \approx 0.924$ is the value of argument at which Dawson's integral attains the maximum.)

The above limiting values are shown in figure 6 by dotted (τ and $N_{\rm aw}$) and dashed–dotted (Φ_∞) horizontal lines. One can see that the numerical results for finite α conform to the limiting values.

The range of variation of parameter τ is rather narrow: as α increases from very low to very high values, τ decreases from 0.487 to 0.451, i.e. by about 8%. Φ_∞ decreases more significantly, although not dramatically: from -0.854 to -1.26. $\Psi_{\rm iw}$ also decreases significantly but not dramatically, from -0.56 for $\alpha = 0.1$ to -0.89 for $\alpha = 10$. $\Psi_{\rm i\infty}$ increases from -0.14 for small α to very small values for large α. $N_{\rm aw}$ varies quite strongly, from 2 for very small α to 21.3 for $\alpha = 10$.

Let us designate by $V_{\rm i\infty}$ the mean velocity of ions leaving the sheath for the plasma normalized by the Bohm velocity: $V_{\rm i\infty} = n_{\rm a}(0)v_{\rm a}/n_{\rm e\infty}u_{\rm B}$. This quantity may be expressed in terms of the above dimensionless parameters as $V_{\rm i\infty} = \tau\exp(-\Phi_\infty)$. With increasing α, $V_{\rm i\infty}$ increases from 1.14 for very small α to 1.59 for very high α. One can conclude that the ion mean velocity at the sheath edge exceeds the Bohm velocity by up to 59%. In other words, the Bohm criterion in the case of ions moving from the sheath into the plasma is satisfied by a substantial margin, rather than with the equality sign which is usual in the case of conventional sheaths with ions moving from the plasma into the sheath.

5. Concluding remarks

Numerical results confirm the concept of a near-cathode space-charge sheath with ionization of atoms emitted by the cathode surface being a double layer with a potential hump: the mathematical problem is solvable and its solution is unique. The accuracy of the numerical results is about 10%. Although further work in this direction is desired in the future, such accuracy seems to be acceptable at the present stage.

Distributions across the sheath have been calculated of ion, electron and atomic densities, electrostatic potential and electric field. The following integral parameters of the sheath have also been calculated: τ the ratio of characteristic fluxes of the atoms and the ions; Φ_∞ the dimensionless height of the potential hump; $N_{\rm aw}$ the ratio of the atomic density at the cathode surface to the atomic density at the potential maximum; and $\Psi_{\rm iw}$, $\Psi_{\rm i\infty}$ the dimensionless average potential energies with which ions are produced before and after potential maximum, respectively. τ, Φ_∞ and $\Psi_{\rm i\infty}$ represent functions of a single control parameter α and may be taken from figures 6(*a*) and (*b*). $N_{\rm aw}$ and $\Psi_{\rm iw}$ represent functions of α and the dimensionless sheath voltage $\chi = eU/kT_{\rm e}$. However, their dependences on χ are weak under conditions of practical interest, which is attested by plateaus manifested at large negative ξ by curves $N_{\rm a}$ in figure 4 and $\Psi_{\rm i}$ in figure 5(*a*). Neglecting these dependences, one can consider $N_{\rm aw}$ and $\Psi_{\rm iw}$ as functions of a single control parameter α and take them from figure 6(*b*).

The control parameter α, characterizing the squared ratio of the Debye length to the scale of variation of the atomic density, is evaluated in terms of quantities at the point of maximum of potential. In order to make the obtained results practicable, one needs to relate α to a parameter evaluated in terms of quantities at the cathode surface. An appropriate parameter is

$$\alpha_{\rm w} = \frac{v_{\rm a}}{u_{\rm B}}\frac{\varepsilon_0 kT_{\rm e}}{n_{\rm aw}e^2}\left(\frac{k_{\rm i}n_{\rm aw}}{v_{\rm a}}\right)^2. \qquad (21)$$

The relation between α_w and α reads $\alpha_w(\alpha) = \alpha\, N_{aw}(\alpha)$ and may be readily evaluated with the use of data on the dependence $N_{aw}(\alpha)$ shown in figure 6(*b*).

Apart from being of theoretical interest, the model of a near-cathode space-charge sheath with ionization of atoms emitted by the cathode surface is of interest due to its possible applications to discharges burning in cathode vapour, including vacuum arcs. In particular, the above-described calculation data on parameters τ, Φ_∞, N_{aw}, Ψ_{iw}, $\Psi_{i\infty}$ can be used for evaluation of a number of quantities which are essential for understanding and modelling of plasma–cathode interaction in such discharges. One of such quantities is the height of the potential hump, which may be evaluated as $\varphi(0) = -\frac{kT_e}{e}\Phi_\infty$. The charged particle density at the sheath edge may be evaluated as $n_{e\infty} = J_v \exp \Phi_\infty / N_{aw}\tau u_B$. The so-called ion backflow coefficient, which plays an important role in theoretical models of cathode spots in vacuum arcs, is defined as the fraction of atoms emitted by the cathode surface that do not escape into the plasma but rather return to the cathode in the form of ions and may be evaluated as $\mu = 1 - N_{aw}^{-1}$. The average kinetic energy of ions bombarding the cathode surface, which is a parameter playing an important role in understanding thermal balance of cathode spot, may be evaluated as $kT_e(\Psi_{iw} - \Phi_\infty) + eU$. The average kinetic energy of ions leaving the sheath may be evaluated as $kT_e(\Psi_{i\infty} - \Phi_\infty)$. The electric field at the cathode surface, which affects the electron emission current, may be evaluated by means of equation (20).

These results may be readily incorporated into models of near-cathode layers and cathode spots in discharges burning in cathode vapour; e.g. [22]. In addition, these results may be employed for qualitative analysis. For example, it follows from the above results that the height of the potential hump is within the range $(0.85–1.26)kT_e/e$. This value is insufficient to explain the observed velocities of ions in cathode jets of vacuum arcs, in agreement with the belief of many researchers that the main contribution to acceleration of ions is given by the plasma pressure gradient.

As another example, one can consider the ion backflow coefficient: since N_{aw} exceeds 2, it follows from the above results that the ion backflow coefficient exceeds 0.5.

As a further example and in addition to the preceding general conclusion, one can try to extract values of the ion backflow coefficient from available experimental data, for example for copper cathodes, and analyse these values in view of the above results. Estimates made in appendix B with the use of experimental data indicate that $0.65 \lesssim \mu \lesssim 0.81$ for copper cathodes. Note that that these values exceed 0.5, in accordance with the above general conclusion. A graph of α_w as a function of T_w for copper cathodes is shown in figure 7 for several values of T_e. (Here n_{aw} and v_a have been calculated by means of equation (1) with $p_v(T_w)$ evaluated with the use of [23]. k_i was evaluated with the use of formulae [24], which take into account both direct and stepwise ionization.) Horizontal dashed lines in this figure represent values $\alpha_w = 0.11$ and $\alpha_w = 3.4$, which correspond to the above-mentioned lower and upper estimates for the ion backflow coefficient $\mu = 0.65$ and $\mu = 0.81$, respectively. One should conclude that if the cathode surface temperature is, say, 3500 K, then the electron temperature is likely to be between approximately 1.45 and 2.6 eV; if $T_w = 4150$ K, then $1.2\,\text{eV} \lesssim T_e \lesssim 2\,\text{eV}$ etc.

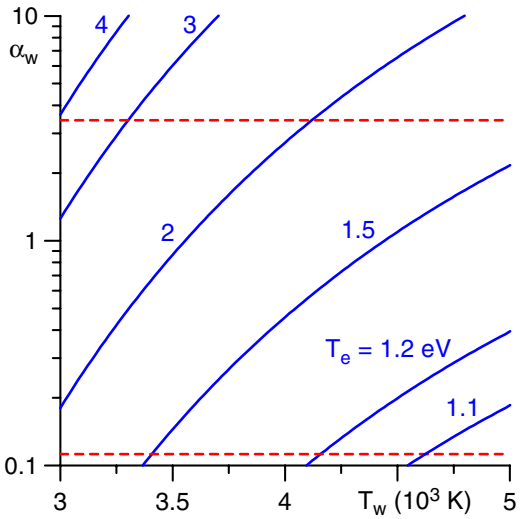

Figure 7. Parameter α_w for a copper cathode.

Acknowledgments

The work was supported by the project PTDC/FIS/68609/2006 of FCT, POCI 2010 and FEDER and by Siemens AG.

Appendix A. Asymptotic behaviour of solution in the vicinity of the maximum of potential

The aim of this appendix is to find asymptotic behaviour of the solution at small ξ, i.e. in the vicinity of the point of maximum of potential. The Taylor expansion of potential $\Phi(\xi)$ at small ξ should read as

$$\Phi(\xi) = -\frac{C_2}{2}\xi^2 + \cdots, \tag{22}$$

where C_2 is a positive constant.

The integrand in equation (10) to a first approximation may be written at small ξ as $\sqrt{2}[C_2(\xi^2 - \zeta^2)]^{-1/2}$. Evaluating the integral, one finds that $N_i(\xi)$ tends at $\xi \to 0$ to a finite value

$$N_i(0) = \frac{\pi\tau}{2\sqrt{C_2}}. \tag{23}$$

Let us substitute expansion (22) into the Poisson equation (9) evaluated at $\xi = 0$. Eliminating C_2 with the use of equation (23), one obtains

$$N_i^3(0) - N_i^2(0) = \frac{\pi^2\alpha\tau}{4}. \tag{24}$$

This is a cubic equation for $N_i(0)$, which admits an analytical solution. The lhs of this equation monotonically increases with an increase in $N_i(0)$ from zero at $N_i(0) = 1$ to infinity at $N_i(0) \to \infty$. One can conclude that this equation is solvable and the solution is unique. Furthermore, $N_i(0)$ is

a monotonically increasing function of a (single) parameter $\alpha\tau$ and

$$N_i(0) \approx 1 + \frac{\pi^2\alpha\tau}{4}, \qquad N_i(0) \approx \left(\frac{\pi^2\alpha\tau}{4}\right)^{1/3} \tag{25}$$

as $\alpha\tau \to 0$ and $\alpha\tau \to \infty$, respectively.

Appendix B. The ion backflow coefficient

The aim of this appendix is to estimate, on the basis of available experimental information, the ion backflow coefficient for the case of copper cathodes. The ion backflow coefficient is defined as the ratio of the number density of flux of nuclei returning from the near-cathode region to the cathode surface to J_v the number density of flux of atoms leaving the cathode surface. If one assumes that the density of flux of atoms returning to the cathode surface is much smaller than density J_{iw} of the ion flux, then $\mu = J_{iw}/J_v$. If one assumes additionally that the plasma in the cathode jet is fully ionized, then $J_v = J_{iw} + \Gamma_i$, where Γ_i is the number density of ion flux from the near-cathode layer into the plasma. The ion backflow coefficient may be expressed as

$$\mu = \frac{\beta_i}{\alpha_i + \beta_i}, \qquad \alpha_i = \frac{e\Gamma_i}{j}, \qquad \beta_i = \frac{eJ_{iw}}{j}, \tag{26}$$

where j is the density of electric current in the near-cathode region.

The experimental value of the ion current in the cathode jets on copper cathodes normalized by the arc current is 0.11 [8, p 157]. Although α_i is defined in terms of current densities rather than integral currents, it seems reasonable to assume $\alpha_i = 0.11$.

Let us proceed to estimation of β_i the fraction of current to the cathode surface which is delivered by ions. An important, if not dominating, contribution to current transfer to cathodes of vacuum arc discharges is delivered by electron emission. Mechanisms considered by different authors include thermo-field emission and explosive electron emission; see, e.g. reviews [2, 8]. The estimates given below refer to the thermo-field emission mechanism.

Electron emission produces a cooling effect over the cathode, since the temperature of the cathode surface inside an operating cathode spot of a vacuum arc exceeds the inversion temperature (although this is not necessarily true during the ignition of a spot). The transition of the cathode material into the gas phase (vaporization) also produces a cooling effect. There should be a mechanism responsible for overcoming the cooling mechanisms and heating the cathode surface up to temperatures necessary for electron emission. A role of such mechanism can be played by heating of the cathode by ions coming from the plasma and accelerated in the space-charge sheath. Therefore, the ion current at the cathode surface must not be too low.

Let us recast this reasoning into a quantitative form. The power balance of the cathode surface may be approximately written as

$$\frac{j_i}{e}(eU - \Delta A) + \frac{j_i}{e}(A_i - A_{eff}) = \frac{j - j_i}{e}A_{eff} + A_vG + q, \tag{27}$$

where A_i is the ionization energy, A_f is the work function, A_{eff} is the effective work function, $\Delta A = A_f - A_{eff}$, $j_i = eJ_{iw}$ is the density of ion current from the near-cathode plasma to the cathode surface, $j - j_i$ represents the density of electric current to the cathode surface transported by the electrons (i.e. the difference between the electron emission current density and the density of current of fast plasma electrons capable of overcoming the repelling electric field in the sheath and reaching the cathode surface), A_v is the vaporization energy per atom, G is the number density of net flux of nuclei leaving the cathode surface and q is the density of flux of heat conduction from the cathode surface into the cathode bulk.

The first term on the lhs of equation (27) accounts for the kinetic energy brought to the cathode by the ions, which come to the cathode surface after having been accelerated by the sheath electric field. The second term accounts for the energy released at the cathode surface as a result of neutralization of the ions. The first term on the rhs accounts for the energy taken away from the cathode by the electrons leaving the cathode for the plasma. The term A_vG accounts for the energy taken away from the cathode by the nuclei leaving the cathode for the plasma. The last term of the rhs accounts for the energy removed from the cathode surface into the cathode bulk by heat conduction. In summary, equation (27) describes balance between the power delivered to the cathode surface by the incident ions, the power removed by the electrons and nuclei leaving the cathode surface, and the power removed by heat conduction into the bulk of the cathode. Obviously, this equation is written in a very simplified form. In particular, it bears no account of terms of the order of thermal energies of electrons and heavy particles and of cooling of the cathode surface by radiation. However, this equation is sufficiently accurate for estimates.

Equation (27) may be solved for fraction of the ion current:

$$\beta_i = \frac{A_{eff} + \tilde{g}A_v + eU_h}{eU + A_i - A_f + A_{eff}}, \tag{28}$$

where $\tilde{g} = eG/j$ is the number of atoms lost by the cathode per elementary charge transported and $U_h = q/j$ is the so-called heating voltage. Note that $\tilde{g}$ may be expressed as $\tilde{g} = eg/m_i$, where g is the erosion rate defined as the loss of mass of the cathode per unit charge transported.

The usual value of 4.5 eV is assumed for the work function A_f of copper. Evaluation of the effective work function by means of fit formulae which have been derived in [25] on the basis of the Murphy–Good formalism [26] shows that $A_{eff} = 3$ eV is a reasonable approximation in the range of T_w of interest. The latent heat of vaporization of copper at the boiling point equals 305 kJ mol^{-1} [23], which corresponds to vaporization energy per atom of 3.16 eV.

Let us assume for estimates $U = 15$ V. Values of erosion rate for copper given by different authors are in the range $g = 50$–$200\,\mu$g C^{-1} (e.g. [27, p 210]), which corresponds to $\tilde{g} = 0.08$–0.3 atoms per electron. The heating voltage may be estimated as $U_h = Q/I$, where Q is the total heat removed by heat conduction into the cathode bulk from a single spot and I is the current per spot. Values of this quantity that can be derived from the literature vary significantly: U_h is close to 1 V in a

wide range of spot currents according to calculations [28] and is approximately 6.3 V according to data cited in [4, p 228]. Given this scatter, the estimates will be done for $\tilde{g} = 0.08$, $U_h = 1$ V, which will give a lower estimate of β_i, and for $\tilde{g} = 0.3$, $U_h = 6.3$ V, which will give a higher estimate.

Substituting the above values into equation (28), one obtains $\beta_i = 0.20$ and $\beta_i = 0.48$ as the lower and higher estimates. Values of the ion backflow coefficient, given by equations (26), are $\mu = 0.65$ and $\mu = 0.81$, respectively.

References

[1] Plyutto A A, Ryzhkov V N and Kapin A T 1965 *Sov. Phys.—JETP* **20** 328–37
[2] Beilis I I 2009 *Plasma Sources Sci. Technol.* **18** 014015
[3] Afanas'ev W P, Djuzhev G A and Shkol'nik S M 1989 *The hydrodynamic model of a plasma jet of a cathode spot in vacuum arc, Preprint of the A. F. Ioffe Physical-Technical Institute No 1375* A F Ioffe Physical-Technical Institute, Leningrad (in Russian)
[4] Beilis I 1995 *Handbook of Vacuum Arc Science and Technology: Fundamentals and Applications* ed R L Boxman *et al* (Park Ridge, NJ: Noyes Publications) pp 208–56
[5] Benilov M S 2010 *J. Phys. D: Appl. Phys.* **43** 175203
[6] Bohm D 1949 *The Characteristics of Electrical Discharges in Magnetic Fields* ed A Guthrie and R K Wakerling (New York: McGraw-Hill) pp 77–86
[7] Riemann K-U 1989 *IEEE Trans. Plasma Sci.* **17** 641–3
[8] Anders A 2008 *Cathodic Arcs: From Fractal Spots to Energetic Condensation* (*Springer Series on Atomic, Optical, and Plasma Physics*) (New York: Springer)
[9] Ecker G 1980 *Vacuum Arcs: Theory and Application* ed J M Lafferty (New York: Wiley) pp 228–320
[10] Almeida N A, Benilov M S and Naidis G V 2008 *J. Phys. D: Appl. Phys.* **41** 245201
[11] Bolotov A V, Kozyrev A V and Korolev Yu D 1993 *Fiz. Plasmy* **19** 709–19 (in Russian)
[12] Bolotov A, Kozyrev A and Korolev Yu 1995 *IEEE Trans. Plasma Sci.* **23** 884–92
[13] Prewett P D and Allen J E 1976 *Proc. R. Soc. Lond.* A **348** 435–46
[14] Franklin R N 1976 *Plasma Phenomena in Gas Discharges* (Oxford: Clarendon)
[15] Tonks L and Langmuir I 1929 *Phys. Rev.* **34** 876–922
[16] Lieberman M A and Lichtenberg A J 2005 *Principles of Plasma Discharges and Material Processing* 2nd edn (New York: Wiley)
[17] McCullen J D, Montierth L M, Morse R L and Neuman W A 1989 *Phys. Fluids* B **1** 448–67
[18] Montierth L M, Morse R L and Neuman W A 1989 *Phys. Fluids* B **1** 1911–25
[19] Krasheninnikov S I and Chodura R 1994 *Contrib. Plasma Phys.* **34** 210–5
[20] Riemann K-U 2006 *Phys. Plasmas* **13** 063508
[21] Harrison E R and Thompson W B 1959 *Proc. Phys. Soc.* **74** 145–52
[22] Benilov M S and Benilova L G 2010 *Proc. 24th Int. Symp. on Discharges and Electrical Insulation in Vacuum (Braunschweig, Germany, 30 August–3 September 2010)* (Germany: TU Braunschweig) submitted
[23] Gale W F and Totemeier T C (ed) 2004 *Smithells Metals Reference Book* 8th edn (Amsterdam/Boston: Elsevier Butterworth-Heinemann)
[24] Benilov M S and Naidis G V 1998 *Phys. Rev.* E **57** 2230–41
[25] Paulini J, Klein T and Simon G 1993 *J. Phys. D: Appl. Phys.* **26** 1310–5
[26] Murphy E L and Good R H 1956 *Phys. Rev.* **102** 1464–73
[27] Farrall G A 1980 *Vacuum Arcs: Theory and Application* ed J M Lafferty (New York: Wiley) pp 184–227
[28] Benilov M S 1993 *Phys. Rev.* E **48** 506–15